narra j

Original Article

Ginger ring compounds as an inhibitor of spike binding protein of alpha, beta, gamma and delta variants of SARS-CoV-2: An *in-silico* study

Tarique N. Hasan[1,2*], Syed S. Naqvi[1], Mati Ur Rehman[1,3], Rooh Ullah[1], Muhammad Ammad[1], Narmeen Arshad[1], Qurat Ul Ain[1], Shabana Perween[1] and Arif Hussain[2]

[1]Pure Health Laboratory, Mafraq Hospital, Abu Dhabi, United Arab Emirates; [2]School of Life Sciences, Manipal Academy of Higher Education, Dubai, United Arab Emirates; [3]College de Paris, France

*Corresponding author: tariquenh@gmail.com

Abstract

The available drugs against coronavirus disease 2019 (COVOD-19), caused by severe acute respiratory syndrome coronavirus 2 (SARS-CoV-2), are limited. This study aimed to identify ginger-derived compounds that might neutralize SARS-CoV-2 and prevent its entry into host cells. Ring compounds of ginger were screened against spike (S) protein of alpha, beta, gamma, and delta variants of SARS-CoV-2. The S protein FASTA sequence was retrieved from Global Initiative on Sharing Avian Influenza Data (GISAID) and converted into ".pdb" format using Open Babel tool. A total of 306 compounds were identified from ginger through food and phyto-databases. Out of those, 38 ring compounds were subjected to docking analysis using CB Dock online program which implies AutoDock Vina for docking. The Vina score was recorded, which reflects the affinity between ligands and receptors. Further, the Protein Ligand Interaction Profiler (PLIP) program for detecting the type of interaction between ligand-receptor was used. SwissADME was used to compute druglikeness parameters and pharmacokinetics characteristics. Furthermore, energy minimization was performed by using Swiss PDB Viewer (SPDBV) and energy after minimization was recorded. Molecular dynamic simulation was performed to find the stability of protein-ligand complex and root-mean-square deviation (RMSD) as well as root-mean-square fluctuation (RMSF) were calculated and recorded by using myPresto v5.0. Our study suggested that 17 out of 38 ring compounds of ginger were very likely to bind the S protein of SARS-CoV-2. Seventeen out of 38 ring compounds showed high affinity of binding with S protein of alpha, beta, gamma, and delta variants of SARS-CoV-2. The RMSD showed the stability of the complex was parallel to the S protein monomer. These computer-aided predictions give an insight into the possibility of ginger ring compounds as potential anti-SARS-CoV-2 worthy of in vitro investigations.

Keywords: Ginger, spike protein, docking, COVID-19, ligands, SARS-CoV-2

https://narraj.org/

Introduction

During 2002–2004 and 2012, two emerging zoonotic diseases, namely severe acute respiratory syndrome (SARS) and Middle East respiratory syndrome (MERS), emerged in humans causing respiratory syndrome [1]. These respiratory diseases are major public health concerns of the 21st century [2]. In late 2019, a new type of coronavirus (severe acute respiratory syndrome

Received: November 17, 2022 - Accepted: February 1, 2023 - Published online: February 13, 2023

coronavirus 2, SARS-CoV-2) emerged in Wuhan, China, causing severe viral pneumonia [1]. More than 6.7 million individuals have died from COVID-19 as of 1 February 2023 [3]. The presence of the virus is abundant in various epithelial tissues, especially in respiratory cells, cardiac cells, and cholangiocytes, where it is found to interact with several host proteins [2].

SARS-CoV-2 is genetically different from other viruses but has 80% similarity to severe acute respiratory syndrome coronavirus 1 (SAR-CoV-1) and 96.2% similarity to bat coronavirus [2]. During the COVID-19 pandemic, multiple mutations appeared in the SARS-CoV-2 genome, and the main variants changed over time [4]. It develops into severe infection consequentially leading to lung injuries with no precise preventive and therapeutic options. There are some variants of concerns (VOC) of SARS-CoV-2 including alpha, beta, delta and gamma commonly referred to as 20I, 20H, 20J, and 21A clades, respectively (Pango lineage-B.1.1.7, B.1.351, P.1 and B.1.617.2), which had been reported having high fatality [2]. Alpha, beta, delta, and gamma variants are more dangerous than the wild-type in terms of morbidity, ICU admission, hospitalization, and mortality [5].

The genome of SARS-CoV-2 encodes 29 proteins. Spike (S) protein is highly conserved among all human coronaviruses and it is found to be involved in various functions including receptor recognition, viral attachment, and host cell entry [5]. S protein functions in the form of trimer, having S1 and S2 subunits containing receptor binding protein (RBD) which in turn binds with angiotensin converting enzyme - 2 (ACE-2) — a crucial cellular receptor abundantly present in epithelial cells of numerous organs [6]. S2 subunit is considered as highly conserved in SARS-CoV-2, hence can be targeted as antiviral drug target [7]. S protein is synthesized as monomer on the host ribosome in cytoplasm of human epithelial cell [4]. Then the monomer attains tertiary structure. If a drug-like molecule is bind to S proteins before the assembly, it may alter their structure, leading to impaired function of S protein.

There are limited treatments that have been demonstrated to be effective against COVID-19 [3]. The development of effective intervention strategies is dependent on understanding of the molecular and cellular mechanisms of SARS-CoV-2 infections, highlighting the importance of studying virus–host interactions at the molecular level [8]. The discovery of SARS-CoV-2 and other coronavirus protein interactions will aid future preparedness and tactics to coronavirus infections [9,10].

Ginger (Zingiberales) is being cultivated for ornamental and medicinal purposes. Moreover, it has been used for centuries as spice [11]. Ginger is an essential component of Indian [12] and Chinese Traditional Medicine [13]. Ginger has been used to treat ailments caused by cold and damp weather. It has also been used as a digestive aid and antinausea remedy, as well as to treat bleeding disorders, rheumatism, baldness, toothache, snakebite, common cold, cough, fever, and respiratory conditions [14]. The curative effect of ginger is attributed to their drug-like molecules individually or probably synergistically [15]. Hence, we hypothesized that the drug-like molecules of ginger may be involved in interaction with S protein monomer. To determine that, we formulated the present *in silico* study, in which we examined the possibility of drug-like compound of ginger and its interaction with S protein monomers of all four variants of SARS-CoV-2 through molecular docking.

Methods

Data source

To obtain proteins of alpha, beta, delta and gamma of SARS-CoV-2, NCBI and GISAID databases were accessed [16-19]. Initially, VOC were obtained from GISAID and then S protein sequence was retrieved from NCBI [20]. Clades of VOC were reconfirmed using Nextstrain [21].

GISAID

All whole genome sequences of alpha, beta, delta and gamma SARS-CoV-2 variants were obtained from GISAID by adding specific filters [22]. To obtain SARS-CoV-2 alpha variant, the “VOC alpha 202012/01 GRY (B.1.1.7) first detected in UK” filter was used, retrieving the most suitable sequence (GISAID ID-EPI_ISL_2803305) [23, 24]. Similarly, beta, gamma, and delta variant

was retrieved from GISAID database using "VOC beta GH/501Y.V2 (B.1.351) first detected in South Africa" (GISAID ID-EPI_ISL_2803657); VOC gamma GR/501Y.V3 (P.1) first detected in Brazil/Japan" (GISAID ID-EPI_ISL_2803309); and "VOC delta G/478K.V1 (B.1.617.2+AY.1+AY.2) first detected in India" (GISAID ID-EPI_ISL_2803744) filters, respectively [25].

NCBI and Nextclade

After retrieving the sequences from GISAID database, each sequence was run on NCBI BLAST to obtain the respective FASTA sequences of S proteins [19]. The FASTA sequences for alpha, beta, delta and gamma were downloaded using GenBank ID: QVW40780.1, QVV20437.1, QTY51296.1, QWO21405.1, respectively [26]. Each sequence obtained from NCBI was run on Nextclade to determine they were originally present in the respective clades (i.e., 20I-α, 20H-β, 20J-γ and 21A-δ) [27]. The FASTA sequences obtained from NCBI were used to develop the ".pdb" format of S protein using Open Babel program (version: 2.4.1) [28, 29].

Druglikeness and ginger compounds selection

To obtain the ginger ring compounds various databases were surveyed including FooDB, FoodComEx, Exposome explorer, PhytoHub, FoodData Central, and Food Composition databases [30]. From 306 ginger compounds, 38 ring containing molecules were selected and enlisted to acquire unique canonical SMILES using PubChem database [31, 32]. Further, SwissADME was used to compute absorption, distribution, metabolism, and excretion (ADME) parameters, pharmacokinetic characteristics, and drug-like performance [33, 34].

Compounds were further screened with following five criteria: (i) high gastrointestinal absorption; (ii) bioavailability score ≥ 0.5; (iii) lipophilicity (octanol–water partition coefficient, $K_{o/w}$) ≤ 5.0; (iv) solubility in water; and (v) not violating any Lipinski's rule [18, 35-37]. Based on above criteria, only 19 compounds were further studied. L-tyrosine also fits in the above criteria but it was not used for downstream works because it was commonly and abundantly available in many food types [38].

Compounds canonical SMILES were used to obtain 3D structure coordinates in ".pdb" format using Open Babel program (version 2.4.1) in order to perform the docking analysis of targeted S protein with filtered ginger compound ligands [39].

Molecular docking

Molecular docking was performed using CB Dock server adopting blind approach [40, 41]. CB Dock was exploited to predict the ligand binding sites to S protein monomer (further in text called as S protein) [42]. The program exploits the local topographies of protein-ligand docking process which automatically recognizes binding sites, analyses the center and size, customizes docking box size according to query ligands, and then execute molecular docking with AutoDock Vina [43].

The docking process uses curvature-based cavity detection approach, hence improving the accuracy of prediction [20, 44]. Suitability of a compound to be a good drug candidate, largely depends on higher binding scores with the target protein. Higher binding scores are mostly based on the function of (i) the number of amino acids involved in formation of binding sites; (ii) the position and size of binding site; and (iii) the type of bonds or interactions involved (such as covalent bond, hydrogen bond, hydrophobic interactions and other weak forces). By considering the fact that if compound is able to bind with protein at or near to the native binding site, then it can alter the native binding site and may not allow the native ligand to bind with protein [45].

Selection on the basis of binding affinity (Vina score) and number of amino acids involved

Docking using CB Dock generated multiple protein-ligand complex models along with the amino acid involved and the Vina score. The selection of the model was based on Vina score (binding affinity) and the number involved amino acids (>20). This selection criteria were implemented for each compound docked with each S protein (alpha, beta, gamma and delta) monomers.

Selection of compounds based on the position of binding sites

Further, each compound-S protein complex model was visualized on the CB Dock to locate the position of binding site. The compounds-S protein complex models with interactions located at or near receptor-binding domain and/or N-terminal domain were selected. This was based on the stipulation that if a compound binds at or near those part of S protein monomer, it will contribute more in the alteration of native binding sites or formation of active trimer [46].

Selection on the basis of hydrogen bonds

At least one hydrogen bond involved in the interaction between the compound and protein was set as criteria to select compounds-S protein complex models. In order to visualize the bonds each protein-compound complex was uploaded to Protein Ligand Interaction Profiler (PLIP) server webpage [47]. The hydrogen bonds were retrieved to observe the rigidity of the complex and specificity to intermolecular interactions [48, 49].

Swiss PDB Viewer (SPDBV) and energy minimization calculation

The calculation of the energy of compound-S protein complex was subjected to Swiss PDB Viewer (SPDBV V 4.1). Energy minimization was also performed for each complex to record the energy from the most stable form [50, 51]. The minimized energy was compared with original force field energy of the complex. This step aimed to evaluate the accuracy of molecular/atomic in the compound-S protein complex generated through the molecular docking [52-54].

Molecular dynamic simulation and RMSD and RMSF calculation

Further, molecular dynamic studies were carried out to map structural divergence of compound-S protein complex as compared to the original form (complex after docking) over time and; the most mobile region/average molecular structure of the complex [55]. The root-mean-square deviation (RMSD) and root-mean-square fluctuation (RMSF) were calculated. For RMSD and RMSF, the calculations were performed on myPresto v5.0–a standalone software. During the molecular dynamic simulation, Loop Limit of 5000 and Generalize Born method were made for the Global minimization. Global Dynamics (molecular dynamic simulation) was performed with molecular dynamic Loop Limit of 1,500,000, where the initial and constant temperatures were set at 300^{o} K and time – 2 femtoseconds. All of other parameters were kept as default [55].

Results

S gene nucleotide and S protein amino acid sequence

Nucleotide and amino acid sequences of alpha, beta, gamma and delta of S protein monomer were obtained using NCBI database and GenBank and all the nucleotide sequences and corresponding amino acid sequences IDs are enlisted in **Table 1**. In addition, these sequences were reversely checked for their corresponding clades using Nextclade, which was also performed for the identification of variation between individual sequence and Wuhan's clade sequence (considered as reference). The data fetched from Nextclade confirmed the clades. Number of mutations in each variant is presented in **Table 1**.

Table 1. Confirmation of the nucleotide sequence based on Nextclade and the number of mutations as compared with the Wuhan's clade sequence

Nucleotide sequence ID (NCBI)	Amino acid FASTA sequence ID(GenBank)	Clade (Nextclade)	Number of mutations (Nextclade)
MZ368185.1	QVW40780.1	20I (Alpha)	38
MW963206.1	QVV20437.1	20H (Beta)	33
MZ294189.1	QWO21405.1	20J (Gamma)	27
MZ284870.1	QTY51296.1	21A (Delta)	33

Druglikeness and ADME evaluation

All the 19 selected compounds along with their respective SMILES and SwissADME-based physiochemical properties are presented in **Table 2**.

Table 2. Data of ginger ring compounds extracted from SwissADME

No	Name of compound	Canonical SMILES	Physicochemical properties				
			Water solubility	Gastrointestinal absorption	Lipinski	Bioavailability score	Consensus log $P_{o/w}$
1	(R)-oxypeucedanin	CC1(C(O1)COC2=C3C=CC(=O)OC3=CC4=C2C=CO4)C	Moderately soluble	High	Yes; 0 violation	0.55	1.85
2	(S)-[6]-gingerol	CCCCCC(CC(=O)CCC1=CC(=C(C=C1)OC)O)O	Moderately soluble	High	Yes; 0 violation	0.55	3.16
3	[6]-shogaol	CCCCCC=CC(=O)CCC1=CC(=C(C=C1)O)OC	Moderately soluble	High	Yes; 0 violation	0.55	3.11
4	cis-[6]-shogaol	CCCCCC=CC(=O)CCC1=CC(=C(C=C1)O)OC	Moderately soluble	High	Yes; 0 violation	0.55	3.76
5	Gingerenone C	COC1=C(C=CC(=C1)CCC(=O)C=CCCC2=CC=C(C=C2)O)O	Moderately soluble	High	Yes; 0 violation	0.55	3.6
6	Methylisoeugenol	CC=CC1=CC(=C(C=C1)OC)OC	Soluble	High	Yes; 0 violation	0.55	2.78
7	p-coumaric acid	C1=CC(=CC=C1C=CC(=O)O)O	Soluble	High	Yes; 0 violation	0.85	1.26
8	Xanthorrhizol	CC1=C(C=C(C=C1)C(C)CCC=C(C)C)O	Moderately soluble	High	Yes; 0 violation	0.55	4.34
9	Zingerone	CC(=O)CCC1=CC(=C(C=C1)O)OC	Soluble	High	Yes; 0 violation	0.55	1.37
10	6-gingerol	CCCCCC(CC(=O)CCC1=CC(=C(C=C1)O)OC)O	Moderately soluble	High	Yes; 0 violation	0.55	3.13
11	6-dehydroshogaol	CCCCCC=CC(=O)C=CC1=CC(=C(C=C1)O)OC	Moderately soluble	High	Yes; 0 violation	0.55	3.17
12	Ginger oleoresin	COC1=C(C=CC(=C1)C=CC(=O)CC(=O)C=CC2=CC(=C(C=C2)O)OC)O	Moderately soluble	High	Yes; 0 violation	0.55	2.37
13	Gingerenone A	COC1=C(C=CC(=C1)CCC=CC(=O)CCC2=CC(=C(C=C2)O)OC)O	Moderately soluble	High	Yes; 0 violation	0.55	2.93
14	Gingerol	CCCCCC(CC(=O)CCC1=CC(=C(C=C1)O)OC)O	Moderately soluble	High	Yes; 0 violation	0.55	2.43
15	Paradol	CCCCCCCC(=O)CCC1=CC(=C(C=C1)O)OC	Moderately soluble	High	Yes; 0 violation	0.55	3.96
16	1-dehydro-(10) gingerdione	CCCCCCCCCC(=O)CC(=O)C=CC1=CC(=C(C=C1)O)OC	Moderately soluble	High	Yes; 0 violation	0.55	3.88
17	17alpha-ethynylestradiol	CC12CCC3C(C1CCC2(C#C)O)CCC4=C3C=CC(=C4)O	Moderately soluble	High	Yes; 0 violation	0.55	3.04
18	Caffeic acid	C1=CC(=C(C=C1C=CC(=O)O)O)O	Soluble	High	Yes; 0 violation	0.56	0.93
19	Zerumbone	CC1=CCC(C=CC(=O)C(=CCC1)C)(C)C	Soluble	High	Yes; 0 violation	0.55	1.79

All the selected ginger ring compounds had high gastrointestinal absorption. Five out of 19 ginger compounds (methylisoeugenol, p-coumaric acid, zingerone, caffeic acid, and zerumbone) were suggested to soluble in water, while the 14 other compounds – moderately soluble in water. The bioavailability score of the p-courmic acid was 0.85 and the others were ≥ 0.55. The logarithm of *n*-octanol/water partition coefficient (log $P_{o/w}$) is used as one of the standard properties identified by Lipinski in the "rule of 5" for drug-like molecules. Based on predicted consensus of log $P_{o/w}$, all 19 compounds were highly lipophilic. Out of these, 4 compounds were considered ideal for good oral and gastrointestinal absorption: p-coumaric acid, zingerone, zerumbone, and (R)-oxypeucedanin (**Table 2**).

Molecular docking of ginger compounds with S protein monomers of SARS CoV-2 variants

Alpha, beta, gamma and delta variant S protein monomers were docked with 19 ginger ring compounds. Selected compound-S protein complexes were analyzed for their Vina score, the involved amino acids as well as the formation of hydrogen bond interaction. The docking results for the docked ligand-protein complexes comprised of S protein monomers of alpha, beta, gamma and delta variants are presented in **Tables 3**.

Table 3. Ginger ring compounds and monomer S protein complex shows the binding affinity and amino acid interaction for each compound at receptor sites

S protein monomer	Ligand	Vina score (kJ/mol) *	Interacting amino acids	Amino acids with H-bond
Alpha	Gingerol	-8	S172, L176, F175, V126, N121, N99, Y170, L226, V227, V120, E96, R102, R190, I119, G103, I128, 1203, W104, S94, F192, I101, S94, E96	S94, E96
	Gingerenone C	-9.5	Y170, I128, I119, W104, G103, R102, I101, N99, E96, L176, F175, Q173, V126, N121, I203, V227, F194, L226, F192, R190, S172	R190, S172
	6-paradol	-8	L226, R190, V227, I203, F192, L176, F175, S94, E96, F92, N99, V126, Y170, N21, I128, I101, I100, R102, I119, W104, V120, L246, L18	L246, L18
	6-dehydroshogaol	-8.4	Q173, L176, S172, F175, N99, V126, N 121, I119, L100, E96, R102, V120, I101, L226, S94, V227, W104, F192, I203, F92, S94, R190	S94, R190
	Cis-6-shagaol	-8.3	L176, N99, S172, V126, F175, V120, R102, I101, Y170, E96, G103, I128, I110, W104, N121, S94, V227, F92, F192, L226, R190	R190, S172
	Ginger oleoresin	-10	P174, S172, L176, V126, F175, Y170, N121, I100, V120, I128, E96, I101, I119, L226, V227, R190, W104, I203, S94, F192, F92, Q173, N99	Q173, N99
	(S)-[6]-gingerol	-8.2	Q173, S172, L176, I75, N99, V126, N121, Y170, E96, V120, I101, I128, L2261, I119, F192, I203, W104, F192, V227, R190, S94	R190, S94
Beta	(R)-oxypeucedanin	-8	S172, Y170, V126, N121, I128, F175, I176, V120, I119, R102, V227, A226, I1011, I203, E96, F1927, F194, S94, F92, W104, N99, R190	N99, R190
	1-dehydro-(10) gingerdione	-8.1	S172, Y170, Q173, V2271, L.226, V126, I203, V127, F175, I119, N121, T492, V420, R490, W104, F92, R102, S894, I101, E96, I128, S94, E96	S94, E96
	6-dehydroshogaol	-8.5	Y 170, V227, S472, I128, L226, I203, V126, I119, F175, Y128, L176, W104, F192, R102, R190, F92, E96I27, I101, N99, S94	N99, S94

S protein monomer	Ligand	Vina score (kJ/mol) *	Interacting amino acids	Amino acids with H-bond
	6-gingerol	-7.9	F194, H207, F192, I203, R190, L226, E96, V227, M01, W104, M177, G103, R102, L176, F175, I119, V120, N121, I128, V126, N99	N99
	Gingerenone A	-8.1	I203, V227, L226, F194, Y170, I128, F192, S172, I119, F92, W104, V 126, Q173, G103, F175, N121, R190, R102, L176, S94, N99, I101, F79	F79
	Gingerenone C	-9.6	I101, R490, R102, F192, L176, G103, W104, N121, T194, F175, I119, I203, V126, I226, V227, Q173, I128, Y170, E96, N99, R190, S172	R190, S172
	Gingerol	-8	S172, Y170, V126, N121, I128, F175, I176, V12d, I119, R102, N99, V227, A226, I1011, I203, R190, F1927, F194, F92, W104, E96, S94	E96, S94
	Ginger oleoresin	-9.9	S94, N99, I100, I101, L176, F92, F192, N121, Q173, V120, W104, V 126, L226, I119, S172, Y203, I128, V227, Y170, R190, E96, F175	E96, F175
Gamma	Caffeic acid	-6.6	K733, M731, Q774, S730, V729, D775, H1058, G1059, T778, P863, I864, P1057, F782, A1056, L865, S1055, T866, I870, D867, F823, V1060, S94, E96, S190	S94, E96, S190
	Ginger oleoresin	-7.5	L226, I119, W104, S205, V120, V126, G193, K206, E191, N121, I203, R102, I208, S94, L139, I101, N99, E96, F192, I190, V341, S399, N488, Y451	V341, S399, N488, Y451
Delta	Caffeic acid	-6	I128, I119, I201, L224, V126, V120, W104, F173, N121, G103, F190, F92, R102, M179, R198, I101, S94, N99, E96, S203, R188	R188
	Ginger oleoresin	-6.2	L862, L863, F780, I868, T864, T861, K731, V727, V1058, S1053, M729, H1056, P1055, F821, D773, S728, T776, D865, S728, G1057, A1054	D773, S728, T776, D865, S728, G1057, A1054

*CB Dock calculates binding affinity or predicts the binding affinity by using a curvature-dependent surface area model (Cyscore) using previously described method [56].

Ginger ring compounds - alpha variant S protein complexes

Seven compounds, namely gingerol, gingerenone C, paradol, 6-dehydroshogaol, cis-6-shagaol, gingeroleoresin, and (s)-[6]-gingerol, having complexes with S protein monomer of alpha variant were selected for analysis.

Figure 1 shows the amino acid and their side chains involved in interaction with each of the seven compounds. The list of those amino acids has also been presented in **Table 3**. Among those compounds, ginger oleoresin had the best-docked Vina score of -10.0 kJ/mol, followed by gingerenone C, 6-dehydroshogaol, cis-6-shagaol, (S)-[6]-gingerol with Vina scores of -9.5, -8.4, -8.3, and -8.2 kJ/mol, respectively. Gingerol and 6-paradol, had relatively lower Vina scores of -8.0 kJ/mol. Analysis on PLIP server revealed that there were two hydrogen bonds involved in the binding of each compound with the protein. The amino acids involved in hydrogen bond formation for gingerol, gingerenone C, 6-paradol, 6-dehydroshogaol, cis-6-shagaol, gingeroleoresin, and (S)-[6]-gingerol were S94, E96; R190, S172; L246, L18; S94, R190; R190, S172; Q173, N199 and R190, S94, respectively (**Figure 2** and **Table 3**). The position of binding site on monomer for the respective compounds are presented in **Figure 3**.

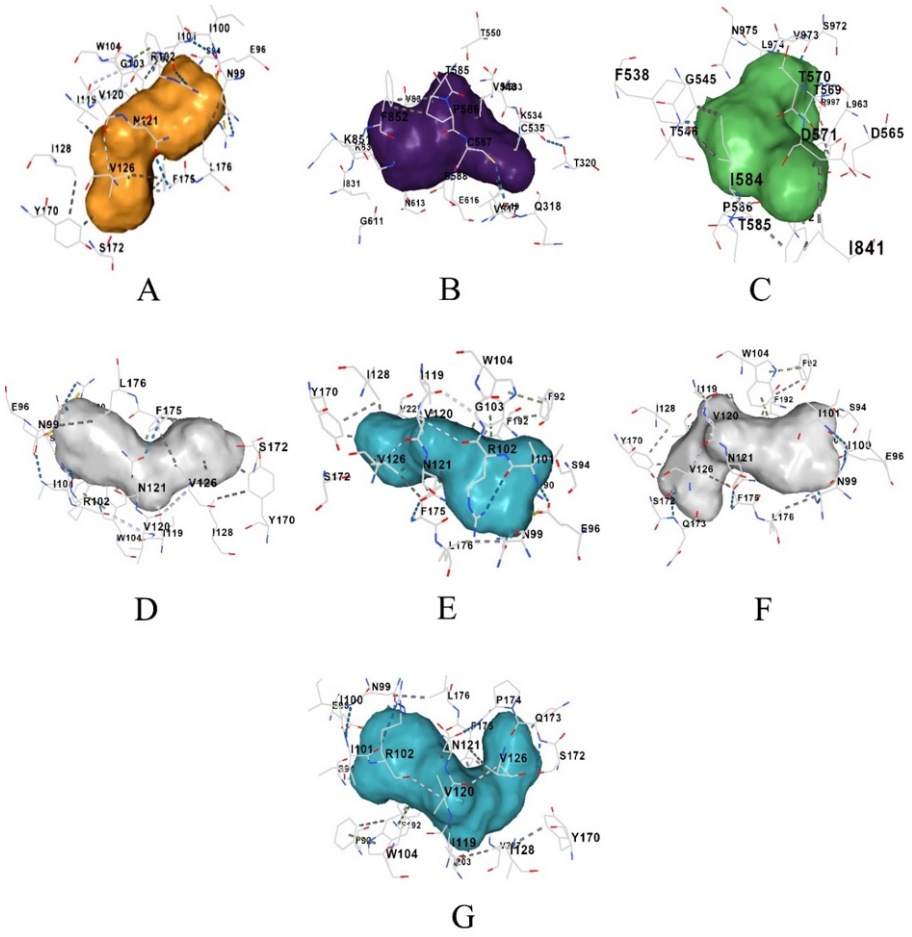

Figure 1. Three dimensional interactions of ligands with alpha monomer of SARS-CoV-2 S protein. (A) gingerol, (B) gingerenone C, (C) 6-paradol, (D) 6-dehydroshogaol, (E) cis-6-shagaol, (F) gingeroleoresin and (G) (S)-[6]-gingerol.

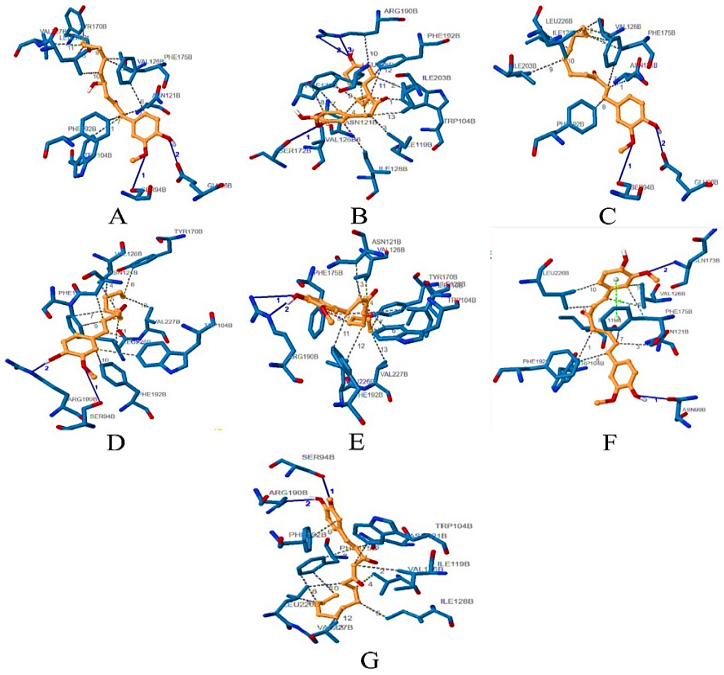

Figure 2. Hydrogen bonding in protein ligand interactions with alpha monomer of SARS-CoV-2 S protein. (A) gingerol, (B) gingerenone C, (C) 6-paradol, (D) 6-dehydroshogaol, (E) cis-6-shagaol, (F) gingeroleoresin and (G) (S)-[6]-gingerol.

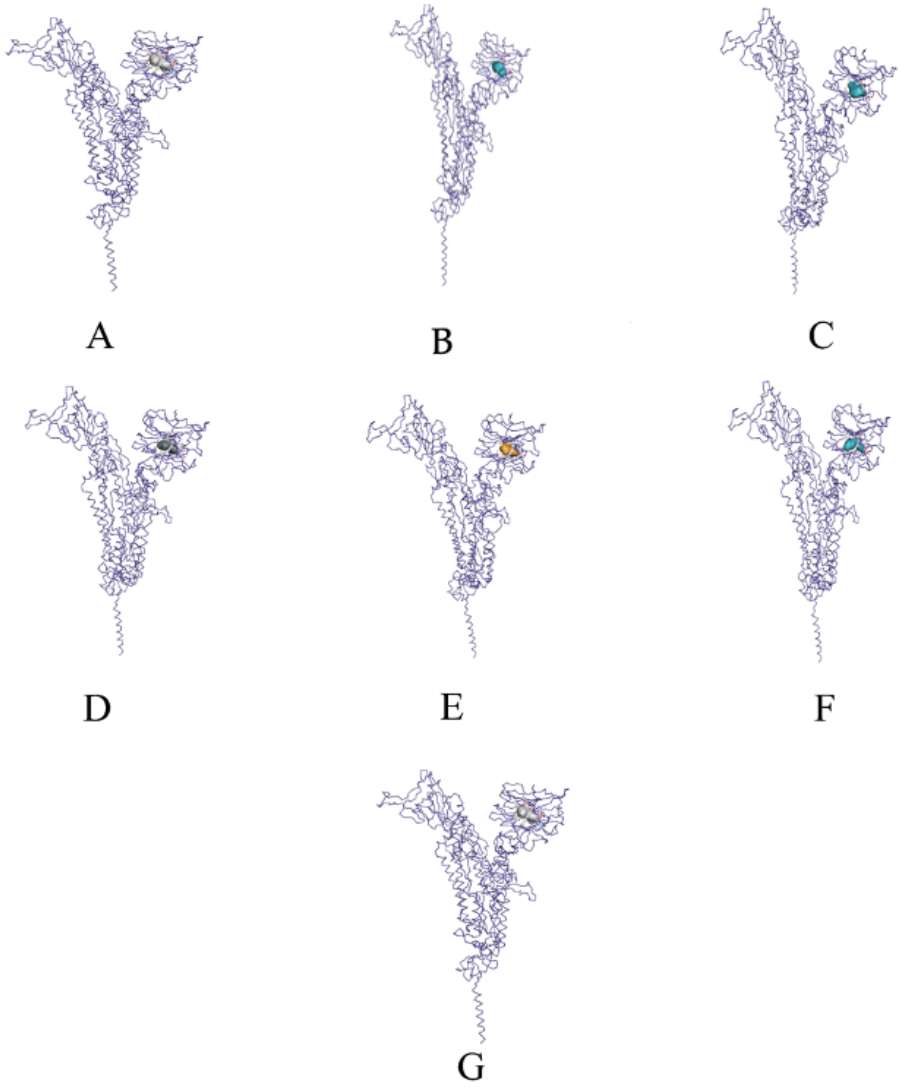

Figure 3. Site of receptor where ligand binds to the monomer of alpha SARS-CoV-2 S protein making protein-ligand complex. (A) gingerol, (B) gingerenone C, (C) 6-paradol, (D) 6-dehydroshogaol, (E) cis-6-shagaol, (F) gingeroleoresin and (G) (S)-[6]-gingerol.

Ginger ring compounds - beta variant S protein complexes

Eight compounds, namely (R)-oxypeucedanin, 1-dehydro-(10) gingerdione, 6-dehydroshogaol, 6-gingerol, gingerenone A, gingerenone C, gingerol, and ginger oleoresin, forming complexes with S protein monomer of beta variant were selected for analysis. **Figure 4** shows the amino acid and their side chains involved in interaction with each of the eight compounds. The list of those amino acids has also been presented in **Table 3**. Among those compounds, ginger oleoresin had the best-docked Vina score of -9.9 kJ/mol, followed by gingerenone C, 6-dehydroshogaol, 1-dehydro-(10) gingerdione, gingerenone A, (R)-oxypeucedanin, gingerol, and 6-gingerol (Vina scores of -9.6, -8.5, -8.1, -8.1, -8.0, -8.0, and -7.9 kJ/mol, respectively). Analysis on PLIP server revealed that there was only one hydrogen bond established in the protein-ligand complex from 6-gingerol and gingerenone A, with amino acids N99 and F79 involved in the interaction. In the case of (R)-oxypeucedanin, 1-dehydro-(10) gingerdione, 6-dehydroshogaol, gingerenone C, gingerol, and ginger oleoresin, two hydrogen bonds were observed with N99, R190; S94, E96; N99, S94; R190, S172; E96, S94; and E96, F175, as contributing amino acids (**Figure 5** and **Table 3**). The binding position on the monomer for the respective compounds are presented in **Figure 6**.

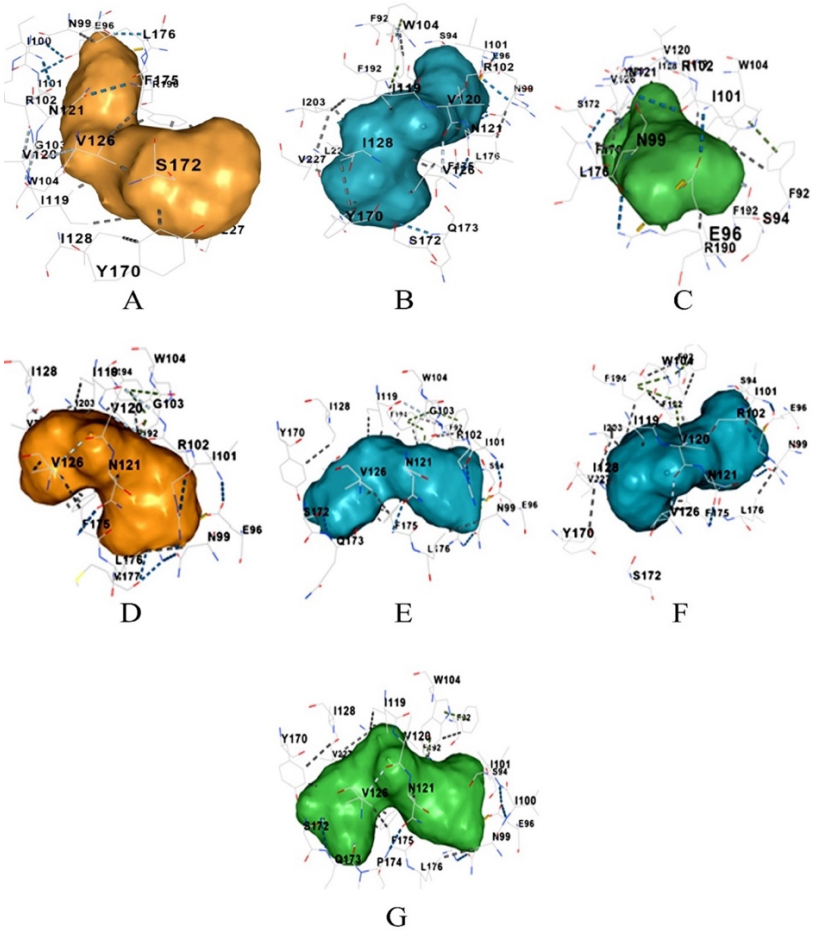

Figure 4. Three dimensional interactions of ligands with beta monomer of SARS-CoV-2 S protein. (A) (R)-oxypeucedanin, (B) 1-dehydro-(10) gingerdione, (C) 6-dehydroshogaol, (D) 6-gingerol, (E) gingerenone A, (F) gingerenone C, and (G) gingerol.

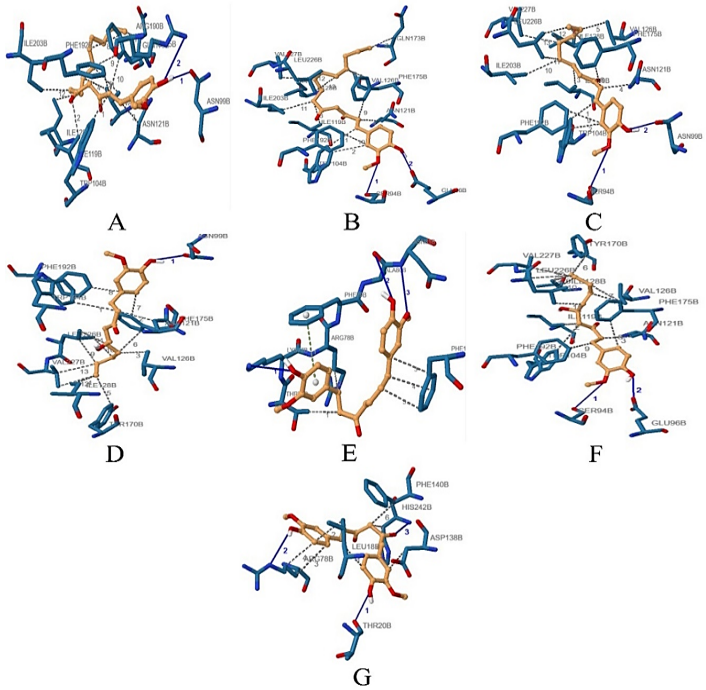

Figure 5. Hydrogen bonding in protein ligand interactions with beta monomer of SARS-CoV-2 S protein. (A) (R)-oxypeucedanin, (B) 1-dehydro-(10) gingerdione, (C) 6-dehydroshogaol, (D) 6-gingerol, (E) gingerenone A, (F) gingerenone C, and (G) gingerol.

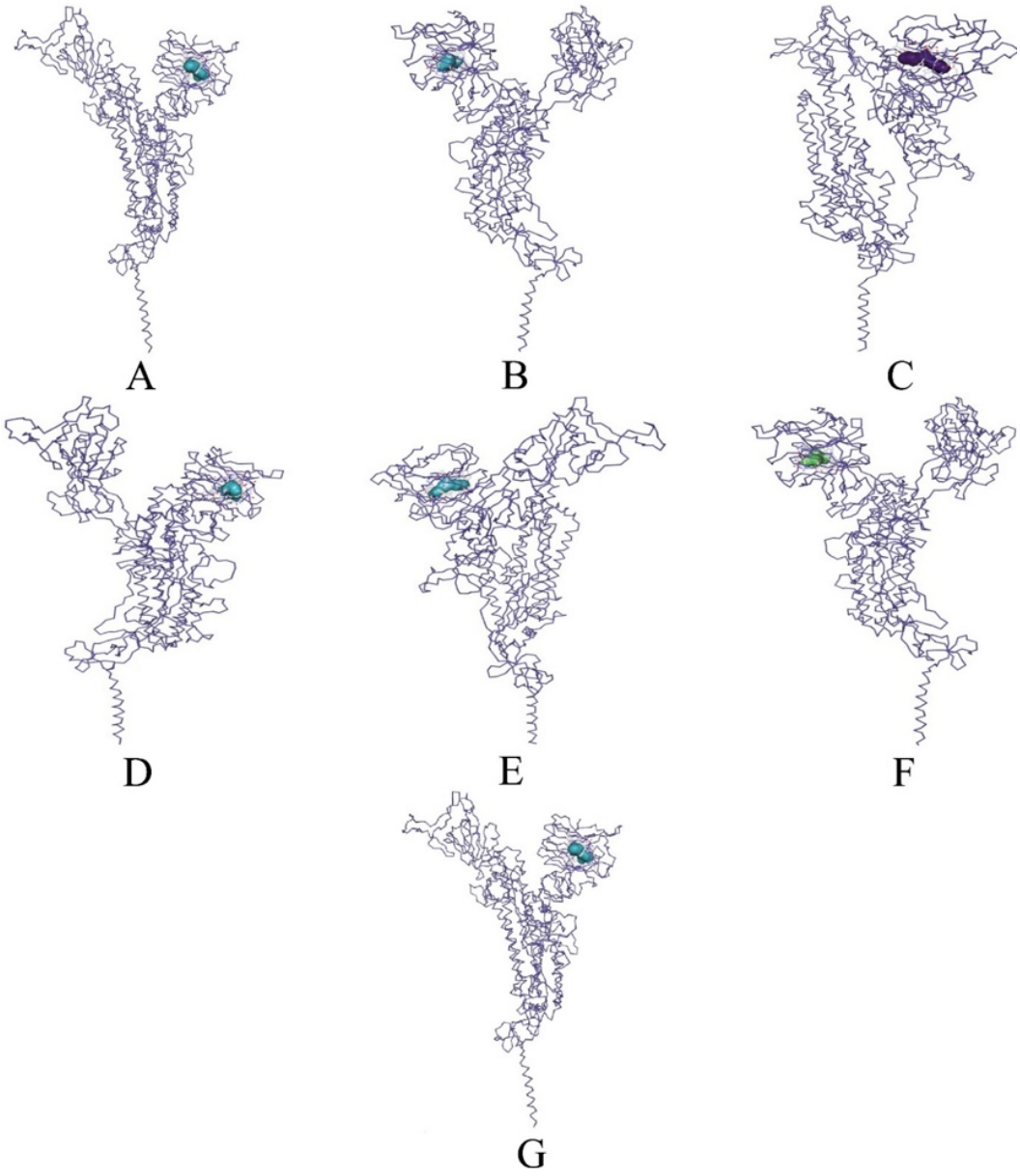

Figure 6. Site of receptor where ligand binds to the beta monomer of SARS-CoV-2 S protein. (A) (R)-oxypeucedanin, (B) 1-dehydro-(10) gingerdione, (C) 6-dehydroshogaol, (D) 6-gingerol, (E) gingerenone A, (F) gingerenone C, and (G) gingerol.

Ginger ring compounds - gamma variant S protein complexes

Two compounds, caffeic acid and ginger oleoresin, that have been docked with the S protein monomer of gamma variant were selected for analysis. **Figure 7** shows the amino acids and their side chains involved in the interaction with each of the two compounds. The list of those amino acids also has been presented in **Table 3**. Among those compounds, ginger oleoresin was found to have the strongest affinity (-7.5 kJ/mol) with the S protein monomer. Meanwhile, caffeic acid yielded a Vina score of -6.6 kJ/mol. Caffeic acid bound to the protein via three hydrogen bonds (out of other interactions) involving amino acids S94, E96 and S190, respectively. As for the ginger oleoresin, there were four hydrogen bonds established by the interaction between the compound and the side chains of amino acids V341, S399, N488 and Y451, respectively. These results could be observed in **Figure 8** and **Table 3**. The position of binding site on S protein monomer for the respective compounds are presented in **Figure 9**.

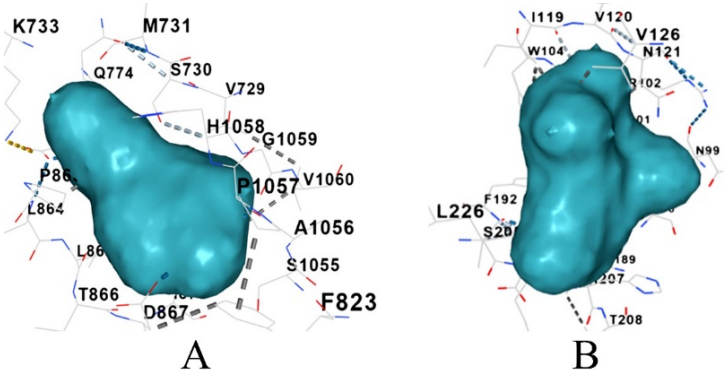

Figure 7. Three dimensional interactions of ligands with gamma monomer of SARS-CoV-2 S protein. (A) caffeic acid and (B) ginger oleoresin.

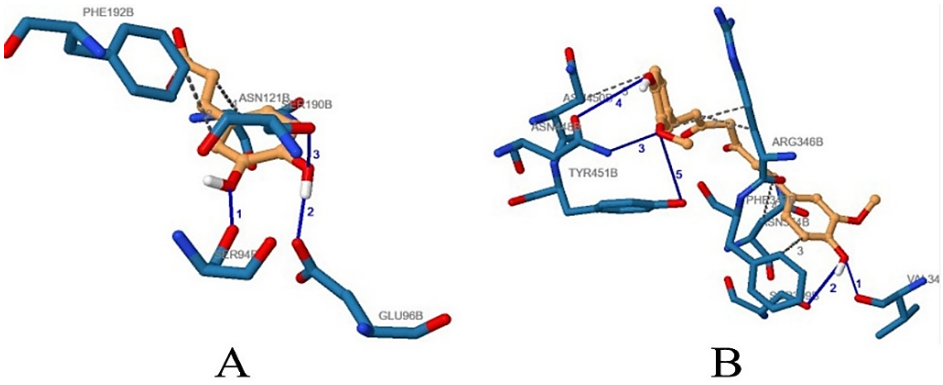

Figure 8. Hydrogen bonding in protein ligand interactions with gamma monomer of SARS-CoV-2 S protein. (A) caffeic acid and (B) ginger oleoresin.

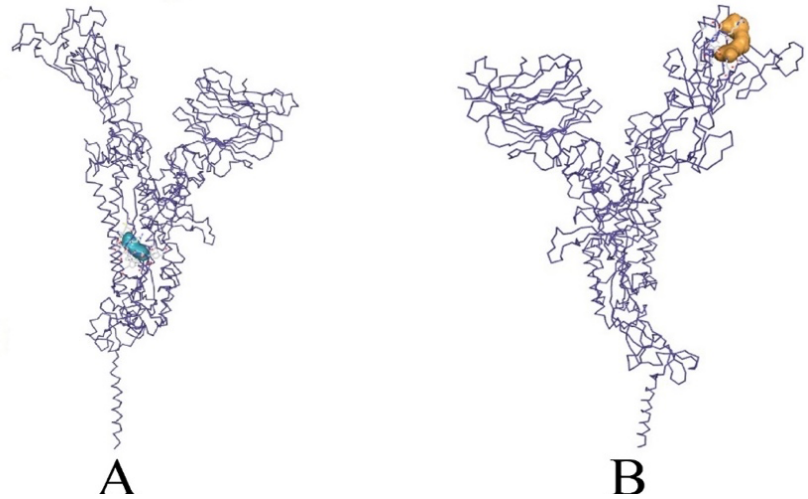

Figure 9. Site of receptor where ligand binds to the gamma monomer of SARS-CoV-2 S protein (A) caffeic acid and (B) ginger oleoresin.

Ginger ring compounds - delta variant S protein complexes

Two compound's, (R)-oxypeucedanin and caffeic acid, complex with S protein monomer of delta variant were selected for analysis. **Figure 10** shows the amino acid and their side chains involved in interaction with each of two compounds. The list of those amino acids is presented in **Table 6**. Among those compounds, caffeic acid had the best-docked Vina score of -6.2, followed by (R)-oxypeucedanin -6.0. There was only one hydrogen bond involved in binding of (R)-oxypeucedanin with involved amino acids as R188 whereas caffeic acid had seven hydrogen bonds with amino acids involved as D773, S728, T776, D865, S728, G1057 and A1054 (**Figure 11** and

Table 6). The position of binding site on monomer for the respective compounds are presented in **Figure 12**.

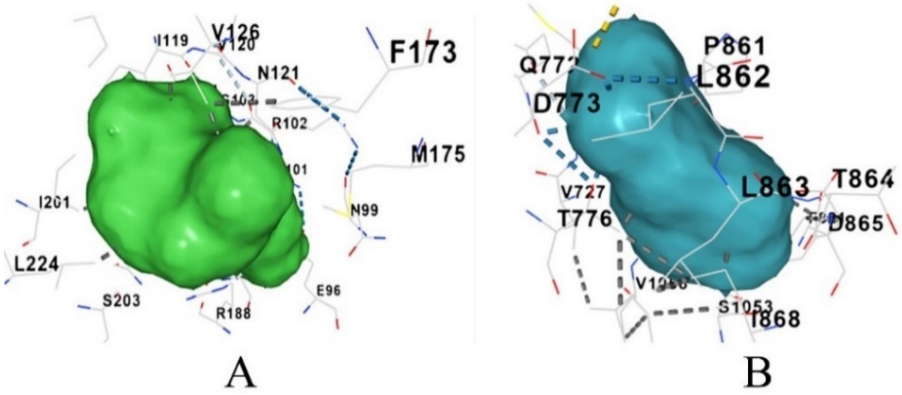

Figure 10. Three dimensional interactions of ligands with delta monomer of SARS-CoV-2 S protein. (A) (R)-oxypeucedanin and (B) caffeic acid.

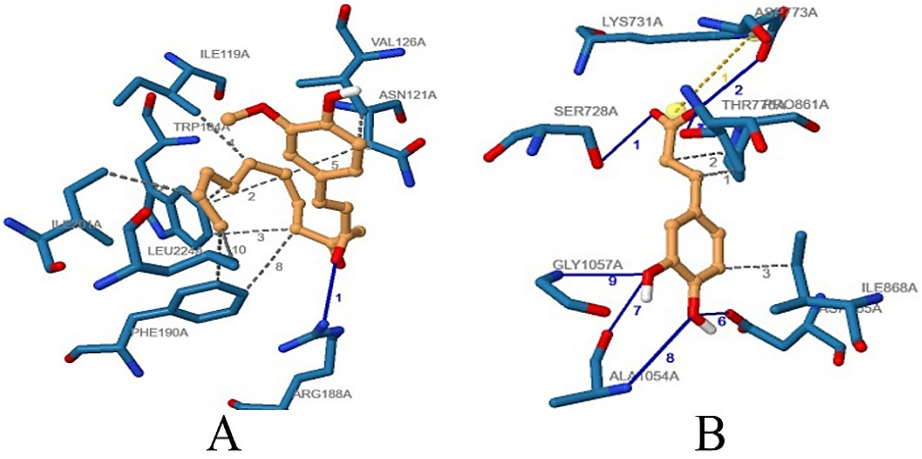

Figure 11. Hydrogen bonding in protein ligand interactions with delta monomer of SARS-CoV-2 S protein. (A) (R)-oxypeucedanin and (B) caffeic acid.

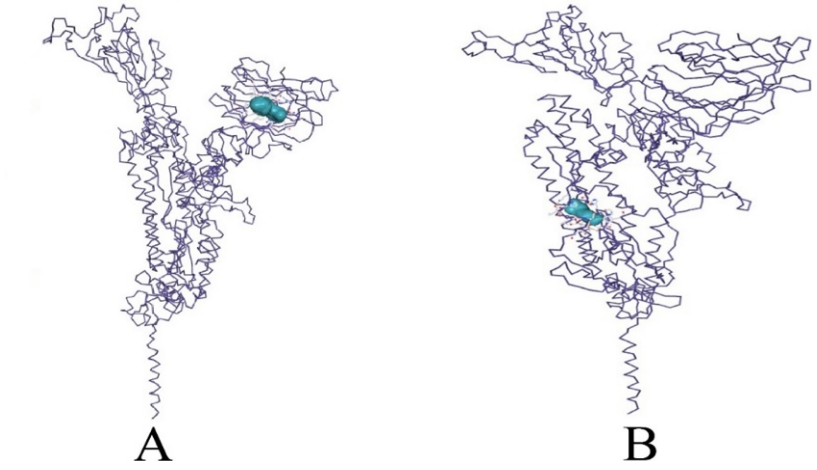

Figure 12. Site of receptor where ligand binds to the delta monomer of SARS-CoV-2 S protein. (A) (R)-oxypeucedanin and (B) caffeic acid.

Energy minimization

Energy minimization of all protein-ligand complexes was conducted using SPDVB. The energy of a protein can be defined as a function of its atomic coordinates, thus providing a quantitative criterion for model selection and refinement. The goal of energy minimization is to find a set of coordinates representing the minimum energy conformation for the given structure. The force field energy obtained for the alpha monomer protein-ligand complex was -48881.6 kJ/mol for all the selected structures. After minimization, the energy obtained was -62477.5 kJ/mol (**Table 4**). The force field energy obtained for beta monomer protein-ligand complex was -48881.6 kJ/mol for all the selected structures. After minimization, the energy obtained was -62477.5 kJ/mol. The force field energies obtained for the complex between gamma monomer protein and caffeic acid and ginger oleoresin were - 50115.9 and -50100.2 kJ/mol, respectively. After minimization, the energy obtained was - 63998.4 and -63982.5 kJ/mol, respectively. The force field energies obtained for Delta monomer protein interacting with (R)-oxypeucedanin and caffeic acid complexes were - 49875.7 and - 49868.5 kJ/mol, respectively. After minimization, the energy obtained was - 63784.3 and - 63779.7 kJ/mol, respectively.

Table 4. Representation of the force field energy with respect to their energy minimization

Variant-S protein monomer	Ligand	Energy (Force Field)	Energy minimized (kJ/mol)
Alpha	6-gingerol	-48881.7	-62477.5
	Gingerenone C	-48866.6	-48867.5
	6-paradol	-48881.7	-62477.5
	6-dehydroshogaol	-48881.7	-62477.5
	cis-6-shagaol	-48881.7	-62477.5
	Ginger oleoresin	-48881.7	-62477.5
	(S)-[6]-gingerol	-48881.7	-62477.5
	Gingerol	-48881.7	-62477.5
Beta	(R)-oxypeucedanin	-48881.7	-62477.5
	1-dehydro-(10) gingerdione	-48881.7	-62477.5
	6-dehydroshogaol	-48881.7	-62477.5
	6-gingerol	-48881.7	-62477.5
	Gingerenone A	-48881.2	-62475
	Gingerenone C	-48866.5	-62463.1
	Gingerol	-48881.2	-62475
	Ginger oleoresin	-48881.2	-62475
Gamma	Caffeic acid	-50115.9	-63998.4
	Ginger oleoresin	-50100.2	-63982.5
Delta	(R)-oxypeucedanin	-49875.7	-63784.3
	Caffeic acid	-49868.5	-63779.7

RMSD calculation

RMSD was calculated for the ginger compounds in their respective binding sites for 3 nanoseconds (**Table 5**). That gives an insight into the stability of intermolecular interaction. Further, this analysis gives perceptions in molecular structure confirmation during simulations, apparently giving an understanding of protein stability and confirming the equilibrium of the simulation.

In alpha monomer complex, RMSD value ranged from $0.166x10^2$ to $0.355x10^2$ nm; beta $0.138x10^2$–$0.263x10^2$ nm; gamma $0.148x10^2$–$0.161x10^2$ nm; and delta $0.149x10^2$–$0.228x10^2$ nm.

RMSF measures the fluctuations of residues during molecular dynamic simulation. The residual fluctuation (RMSF) values are directly dependent on ligand binding energy and interaction. RMSF calculations for each residue are presented in **Table 5**.

In alpha monomer complex, the RMSF values ranged from $0.297x10^2$ to $0.303x10^2$ nm, beta $0.298x10^2$–$0.163x10^7$ nm; gamma $0.298x10^2$–$0.303x10^2$ nm; and delta $0.296x10^2$–$0.245x10^5$ nm.

Table 5. Molecular Dynamics Simulation (RMSD and RMSF calculation) of compounds - S protein monomer complexes

Variant-S protein monomer	Ligand	RMSD (nm)	RMSF (nm)
Alpha	Gingerol	0.234x10²	0.299x10²
	Gingerenone C	0.192x10²	0.297x10²
	6-paradol	0.166x10²	0.301x10²
	6-ehydroshogaol	0.257x10²	0.300x10²
	Cis-6-shagaol	0.355x10²	0.298x10²
	Ginger oleoresin	0.188x10²	0.303x10²
	(s)-[6]-gingerol*	0.193x10²	0.299x10²
Beta	(R)-oxypeucedanin	0.150x10²	0.302x10²
	1-dehydro-(10) gingerdione**	0.141x10²	0.163x10⁷
	6-dehydroshogaol	0.180x10²	0.301x10²
	6-gingerol	0.147x10²	0.298x10²
	Gingerenone A	0.263x10²	0.301x10²
	Gingerenone C	0.214x10²	0.300x10²
	Gingerol	0.138x10²	0.301x10²
	Ginger oleoresin	0.143x10²	0.301x10²
Gamma	Caffeic acid	0.161x10²	0.298x10²
	Ginger oleoresin	0.148x10²	0.303x10²
Delta	(R)-oxypeucedanin***	0.149x10²	0.245x10⁵
	Caffeic acid	0.228x10²	0.296x10²

All ligand-protein complexes were run for 3 nanoseconds in triplicate
* Run only for 230.4 pico-seconds
** Run only for 96 pico-seconds
*** Run only for 971.2 pico-seconds

Discussion

Historically, Coronaviruses is known for causing respiratory, digestive, liver and central nervous system diseases in human [57]. An emerged SARS-CoV-2 caused a pandemic and still acts as one of the serious public health concerns [58]. Their pan global spread among the populations and faster spread of infection in human body is largely attributed by their faster genomic mutation ability [59]. The same has caused the emergence of many VOCs and interest (Vol) [60]. Although the list is changing overtime, four major VOCs have been recorded previously [61]. Due to the lack of any targeted medicine against the virus, the pandemic was primarily managed by prevention of infection, control measures, and supportive care [53]. Hence, this study was designed to identify and characterize the drug-like compounds from a medicinal plant which is already a part of food habit as well as known for its medicinal properties. Particularly, ginger which is used as decoction to cure cold and cough in Unani medicinal system [62]. In this study, the ginger ring compounds were screened for their ability to bind with S protein monomer of all four of SARS CoV-2.

S protein trimer is constituted of S1 and S2 subunits. Meanwhile, S protein (monomer) protomer is comprised of N-terminal domain (NTD), receptor binding domain (RBD), fusion peptide domain (FP), heptad repeat-1 (HR1), and crystallizable domain (CD) [63]. NTD, RBD, FP, and HR-1 of the monomer are involved in constituting S1 and S2 subunits, known for facilitating host receptor identification and membrane penetration [64]. As far as synthesis of monomer occurs in the cytoplasm of host cell, it could be targeted by drug-like compounds [65, 66].

In this present study, SwissADME was applied to study pharmacokinetics of all 38 selected ring compounds from ginger [67]. Among them, 19 were found either soluble or moderately soluble in water with high gastrointestinal absorption, bioavailability ≥ 0.55, lipophilicity ≤ 5 $K_{o/w}$, and zero violation of Lipinski's rule of drug likeness (**Table 2**). Interestingly, the bioavailability score of p-coumaric acid was 0.85. p-Coumaric acid has been studied for its antioxidative, anticancer, and other biological activities [68]. Also, the compound has been reported to attenuate lung inflammation induced by lipopolysaccharides [69]. In our study, p-coumaric was also found to have higher bioavailability score, supporting the idea that the compound is a potential drug candidate against SARS-CoV-2.

In addition, other 18 compounds have bioavailability score ≥ 0.55. However, log $P_{o/w}$ in 5 compounds (R-oxypeucedanin, p-coumaric acid, caffeic acid, zingerone, and zerumbone) are found less than 2; 4 compounds (methyl isoeugenol, ginger oleoresin, gingerenone A, and gingerol) — more than 2; 9 compounds ([S]-[6]-gingerol, [6]-shogaol, 17 alpha-ethynylestradiol, cis-[6]-shogaol, gingerenone C, 6-gingerol, 6-dehydroshogaol, paradol, and 1-dehydro-[10] gingerdione) —more than 3; and 1 compound (xanthorrhizol) — more than 4 (**Table 2**). Most of the above mentioned compounds have been studied for their medicinal properties [70].

Compounds from ginger had been studied and proven in curing the lung abnormalities and respiratory illness. Anti-inflammatory properties of ginger ring compounds enfold relief of respiratory symptoms associated to SARS-CoV-2 [71]. Compounds such as 6-shogaol affects the inflammatory cascade and was found to have anti-platelet properties in vitro [72]. Other medicinal properties of ginger group include improvement in oxygenation [73]. Studies suggest that caffeic acid have potential to obstruct viral 3-chymotrypsin-like cysteine protease ($3CL^{pro}$) enzyme eventually preventing replication of virus and inhibiting viral protease enzyme [74]. Gingerenone A is found to be an inhibitor of JAK2 and p70S6 kinase hence inhibiting the JAK2 activity in replication and assembly of influenza virus [75]. p-Coumaric acid has been found to have immunomodulatory and anti-inflammatory properties in vivo [69]. The 1-dehydro-(10) gingerdione is found to be involved in the regulation of inflammatory genes [76]. Our *in silico* ADME study is in agreement with the findings from various literatures [70-75], where the ADME study suggests the compounds are worthy for further investigation as anti-SARS-CoV-2.

For molecular docking of S protein monomer and ginger compound, CB Dock (online tool) had been used, in which the program utilizes Autodock Vina for docking. It involves automated (binding site) cavity detection (CurPocket) on protein and flexible docking. After docking, the results were enlisted as Vina score, where the function of protein–ligand binding affinity is calculated using a curative-dependent surface area model. All the sorted compounds were docked against S protein monomer of alpha, beta, delta, and gamma variants. Those compounds were selected which either were binding with monomers in a cavity having more than 20 amino acid or Vina score of more than 8 or both. **Table 3** presents those selected compounds binding with alpha, beta, delta, and gamma S protein monomers and also the amino acids involved in the binding sites. As far as the binging of protein and compounds are concerned, exempting covalent bond, that will be more stable with higher number of weak forces (hydrophobic interaction and hydrogen-bonds) between compound molecule and the binding site [77, 78]. Among them, hydrogen bond is the strongest one [73]. In this present study, gingerol; gingerenone C; 6–paradol; 6-dehydroshogaol; cis-6-shagaol; ginger oleoresin; and (s)- [6]-gingerol were found forming interaction with alpha variant S protein monomer with several hydrophobic interactions and 2 hydrogen bonds. Meanwhile, (R)-oxypeucedanin, 1-dehydro-(10) gingerdione, 6-dehydroshogaol, 6-gingerol, gingerenone A, gingerenone C, gingerol, and ginger oleoresin were found binding with beta variant S protein monomer with at least 1–2 hydrogen bonds and several hydrophobic interactions. In the case of gamma variant protein, caffeic acid and ginger oleoresin established interactions with the protein via 3–4 hydrogen bonds, in addition of many other weak interactions. (R)-oxypeucedanin and caffeic acid were shown having 1 and 7 hydrogen bonds, respectively, and other hydrophobic interactions in binding with delta variant S protein monomer (**Table 3**).

Further, the minimum energy was calculated for all the monomer models after removing the interacting compound. That helps to figure out the most stable confirmation of monomer for the foregoing compounds (Ref- Energy minimization using SPDVB). It had been found that upon energy minimization, the change in energy (ΔE) was in a range of 14000 kJ/mol for monomer compound complexes of alpha, beta, gamma, and delta monomers. Inter-molecular confirmational stability of a molecule is a function of RMSD [79]. The monomer confirmation after binding with compounds was not different in RMSD (for alpha, beta, gamma, and delta) as compared with original S protein monomer structure of Wuhan strain [80]. However, the difference in RMSD was recorded among monomer-compound complexes (**Table 5**). As a matter of fact, difference in RMSD suggests the confirmational changes due to interaction

of compound molecules with monomers [77] . The molecular docking programs are used to filter potentially active compounds towards the protein ligand from a large group of compounds [77].

Conclusions

This present study suggests that the lead compounds gingerol, gingerenone C, 6-paradol, 6-dehydroshogaol, cis-6-shagaol, gingeroleoresin, (s)-6-gingerol, (R)-oxypeucedanin, 1-dehydro-(10) gingerdione, 6-gingerol, gingerenone A, and caffeic acid are able to induce the conformational changes while not influencing the stability of S protein monomer of SARS-CoV-2 (alpha, beta delta and gamma variants). That advocates their candidature for further evaluations. In future, studies are needed before they could be established as suitable lead molecule of interest against SARS-CoV-2.

Ethics approval

Not required.

Acknowledgments

All the authors acknowledge and thank their respective institutes and universities. All the authors substantially contributed to the conception, design, analysis and interpretation of data, checking and approving the final version of the manuscript, and agree to be accountable for its contents.

Conflict of interest

All the authors declare that there are no conflicts of interest.

Funding

This study received no external funding.

Underlying data

All data underlying the results are available as part of the article and no additional source data are required.

How to cite

Hasan TN, Naqvi SS, Rehman MU, *et al.* Ginger ring compounds as an inhibitor of spike binding protein of alpha, beta, gamma and delta variants of SARS-CoV-2: An *in-silico* study. Hasan et al. Narra J 2023; 3 (1): e98 - http://doi.org/10.52225/narra.v3i1.98.

References

1. El-Kafrawy SA, Corman VM, Tolah AM, *et al.* Enzootic patterns of Middle East respiratory syndrome coronavirus in imported African and local Arabian dromedary camels: a prospective genomic study. Lancet Planet Health 2019; 3(12):e521-e528.
2. Hu B, Guo H, Zhou P, *et al.* Characteristics of SARS-CoV-2 and COVID-19. Nat Rev Microbiol 2021; 19(3):141-154.
3. Zhou P, Yang X-L, Wang X-G, *et al.* A pneumonia outbreak associated with a new coronavirus of probable bat origin. Nature 2020; 579(7798):270-273.
4. Ghinai I, McPherson TD, Hunter JC, *et al.* First known person-to-person transmission of severe acute respiratory syndrome coronavirus 2 (SARS-CoV-2) in the USA. Lancet 2020; 395(10230):1137-1144.
5. Aanouz I, Belhassan A, El-Khatabi K, *et al.* Moroccan Medicinal plants as inhibitors against SARS-CoV-2 main protease: Computational investigations. J Biomol Struct Dyn 2021; 39(8):2971-2979.
6. Seyran M, Takayama K, Uversky VN, *et al.* The structural basis of accelerated host cell entry by SARS-CoV-2. FEBS 2021; 288(17):5010-5020.

7. Guan W-j, Ni Z-y, Hu Y, *et al*. Clinical characteristics of coronavirus disease 2019 in China. New Engl J Med 2020; 382(18):1708-1720.
8. V' kovski P, Kratzel A, Steiner S, *et al*. Coronavirus biology and replication: implications for SARS-CoV-2. Nat Rev Microbiol 2021; 19(3):155-170.
9. McIntosh K, Hirsch M, Bloom A. Coronavirus disease 2019 (COVID-19): Epidemiology, virology, and prevention. Lancet Infect Dis 2020; 1:2019-2020.
10. Lin L, Liu Y, Tang X, *et al*. The disease severity and clinical outcomes of the SARS-CoV-2 variants of concern. Front Public Health 2021; 9.
11. Bhatt N, Waly MI, Essa MM, *et al*. Ginger: A functional herb. Food as Medicine 2013:51-71.
12. Pandey M, Rastogi S, Rawat A. Indian traditional ayurvedic system of medicine and nutritional supplementation. Evidence-Based Complementary and Alternative Medicine 2013; 2013.
13. Wang W, Wang Z. Studies of commonly used traditional medicine-ginger. Zhongguo Zhongyao Zazhi = China J Chinese Materia Medica 2005; 30(20):1569-1573.
14. Moghaddasi MS, Kashani HH. Ginger (Zingiber officinale): A review. J Med Plants Res 2012; 6(26):4255-4258.
15. Anjorin AA. The coronavirus disease 2019 (COVID-19) pandemic: A review and an update on cases in Africa. Asian Pac J Trop Med 2020; 13(5):199.
16. Cui J, Li F, Shi Z-L. Origin and evolution of pathogenic coronaviruses. Nat Rev Microbiol 2019; 17(3):181-192.
17. De Wit E, Van Doremalen N, Falzarano D, *et al*. SARS and MERS: recent insights into emerging coronaviruses. Nature Rev Microbiol 2016; 14(8):523-534.
18. Liu R, Hu J. Computational prediction of heme-binding residues by exploiting residue interaction network. PloS One 2011; 6(10):e25560.
19. Tan W, Zhao X, Ma X, *et al*. A novel coronavirus genome identified in a cluster of pneumonia cases—Wuhan, China 2019– 2020. China CDC Weekly 2020; 2(4):61-62.
20. Graham RL, Baric RS. Recombination, reservoirs, and the modular spike: mechanisms of coronavirus cross-species transmission. J Virol 2010; 84(7):3134-3146.
21. Gorbalenya AE, Baker SC, Baric R, *et al*. Severe acute respiratory syndrome-related coronavirus: The species and its viruses–a statement of the Coronavirus Study Group. 2020.
22. Lv L, Li G, Chen J, *et al*. Comparative genomic analysis revealed specific mutation pattern between human coronavirus SARS-CoV-2 and Bat-SARSr-CoV RaTG13. Front Microbiol 2020;11:584717.
23. Sevajol M, Subissi L, Decroly E, *et al*. Insights into RNA synthesis, capping, and proofreading mechanisms of SARS-coronavirus. Virus Res 2014; 194:90-99.
24. van Dorp L, Acman M, Richard D, *et al*. Emergence of genomic diversity and recurrent mutations in SARS-CoV-2. Infect Genet Evol 2020; 83:104351.
25. Fauver JR, Petrone ME, Hodcroft EB, *et al*. Coast-to-coast spread of SARS-CoV-2 during the early epidemic in the United States. Cell 2020; 181(5):990-996. e995.
26. Jackson B, Boni MF, Bull MJ, *et al*. Generation and transmission of interlineage recombinants in the SARS-CoV-2 pandemic. Cell 2021; 184(20):5179-5188.
27. Sehra ST, Salciccioli JD, Wiebe DJ, *et al*. Maximum daily temperature, precipitation, ultraviolet light, and rates of transmission of severe acute respiratory syndrome coronavirus 2 in the United States. Clin Infect Dis 2020; 71(9):2482-2487.
28. Babuji Y, Blaiszik B, Brettin T, *et al*. Targeting SARS-CoV-2 with AI-and HPC-enabled lead generation: a first data release. arXiv preprint. arXiv:200602431 2020.
29. Vijgen L, Keyaerts E, Moës E, *et al*. Complete genomic sequence of human coronavirus OC43: molecular clock analysis suggests a relatively recent zoonotic coronavirus transmission event. J Virol 2005; 79(3):1595-1604.
30. Medina-Franco JL, Petit J, Maggiora GM. Hierarchical strategy for identifying active chemotype classes in compound databases. Chem Biol Drug Des 2006; 67(6):395-408.
31. Mahanta S, Chowdhury P, Gogoi N, *et al*. Potential anti-viral activity of approved repurposed drug against main protease of SARS-CoV-2: an in silico based approach. J Biomol Structr Dyn 2021; 39(10):3802-3811
32. Ahkam AH, Hermanto FE, Alamsyah A, *et al*. Virtual prediction of antiviral potential of ginger (Zingiber officinale) bioactive compounds against spike and MPro of SARS-CoV2 protein. Berkala Penelitian Hayati 2020; 25(2):52-57.

33. Ubani A, Agwom F, RuthMorenikeji O, *et al*. Molecular docking analysis of some phytochemicals on two SARS-CoV-2 targets: potential lead compounds against two target sites of SARS-CoV-2 obtained from plants. F1000Research 2020, 9:1157.
34. Ma R-H, Ni Z-J, Zhu Y-Y, *et al*. A recent update on the multifaceted health benefits associated with ginger and its bioactive components. Food & Function 2021; 12(2):519-542.
35. Narkhede RR, Pise AV, Cheke RS, *et al*. Recognition of natural products as potential inhibitors of COVID-19 main protease (Mpro): In-silico evidences. Nat Prod Bioprospect 2020; 10(5):297-306.
36. Temperton NJ, Chan PK, Simmons G, *et al*. Longitudinally profiling neutralizing antibody response to SARS coronavirus with pseudotypes. Emerg Infect Dis 2005; 11(3):411.
37. Chen X, Li H, Tian L, *et al*. Analysis of the physicochemical properties of acaricides based on Lipinski's rule of five. J Comput Biol 2020; 27(9):1397-1406.
38. Lütke-Eversloh T, Santos CNS, Stephanopoulos G. Perspectives of biotechnological production of L-tyrosine and its applications. Appl Microbiol Biotechnol 2007; 77(4):751-762.
39. San Chang J, Wang KC, Yeh CF, *et al*. Fresh ginger (Zingiber officinale) has anti-viral activity against human respiratory syncytial virus in human respiratory tract cell lines. J Ethnopharmacol 2013; 145(1):146-151.
40. Elbe S, Buckland-Merrett G. Data, disease and diplomacy: GISAID's innovative contribution to global health. Global Challenges 2017; 1(1):33-46.
41. Shu Y, McCauley J. GISAID: Global initiative on sharing all influenza data–from vision to reality. Eurosurveillance 2017; 22(13):30494.
42. Hadfield J, Megill C, Bell SM, *et al*. Nextstrain: real-time tracking of pathogen evolution. Bioinformatics 2018; 34(23):4121-4123.
43. Abinaya M, Gayathri M. Inhibition of biofilm formation, quorum sensing activity and molecular docking study of isolated 3, 5, 7-Trihydroxyflavone from Alstonia scholaris leaf against *P. aeruginosa*. Bioorganic Chem 2019; 87:291-301.
44. Oong XY, Ng KT, Takebe Y, *et al*. Identification and evolutionary dynamics of two novel human coronavirus OC43 genotypes associated with acute respiratory infections: phylogenetic, spatiotemporal and transmission network analyses. Emerg Microb Infect 2017; 6(1):1-13.
45. Hasan TN, Masoodi TA, Shafi G, *et al*. Affinity of estrogens for human progesterone receptor A and B monomers and risk of breast cancer: a comparative molecular modeling study. Adv Appl Bioinform Chem 2011; 4:29.
46. Dokainish HM, Re S, Mori T, *et al*. The inherent flexibility of receptor binding domains in SARS-CoV-2 spike protein. Elife 2022; 11: e75720.
47. De Maio N, Walker C, Borges R, *et al*. Issues with SARS-CoV-2 sequencing data. 2020.
48. Guan Q, Guo Y, Sui X, *et al*. Changes in photosynthetic capacity and antioxidant enzymatic systems in micropropagated Zingiber officinale plantlets during their acclimation. Photosynthetica 2008; 46(2):193.
49. Ter Meulen J, Van Den Brink EN, Poon LLM, *et al*. Human monoclonal antibody combination against SARS coronavirus: synergy and coverage of escape mutants. PLoS Med 2006; 3(7):e237.
50. Gao D, Kuang X, Qiao P, *et al*. Molecular characterization and expression analysis of the autophagic gene Beclin 1 from the purse red common carp (*Cyprinus carpio*) exposed to cadmium. Comp Biochem Physiol Part - C: Toxicol Pharmacol 2014; 160:15-22.
51. LaBranche CC, Henderson R, Hsu A, *et al*. Neutralization-guided design of HIV-1 envelope trimers with high affinity for the unmutated common ancestor of CH235 lineage CD4bs broadly neutralizing antibodies. PLoS Pathog 2019; 15(9):e1008026.
52. Bricault CA, Yusim K, Seaman MS, *et al*. HIV-1 neutralizing antibody signatures and application to epitope-targeted vaccine design. Cell Host Microbe 2019; 25(1):59-72. e58.
53. Zhou M, Zhang X, Qu J. Coronavirus disease 2019 (COVID-19): a clinical update. Fronts Med 2020; 14(2):126-135.
54. Sadjadpour R, Donau OK, Shingai M, *et al*. Emergence of gp120 V3 variants confers neutralization resistance in an R5 simian-human immunodeficiency virus-infected macaque elite neutralizer that targets the N332 glycan of the human immunodeficiency virus type 1 envelope glycoprotein. J Virol 2013; 87(15):8798-8804.
55. Kasahara K, Terazawa H, Itaya H, *et al*. myPresto/omegagene 2020: a molecular dynamics simulation engine for virtual-system coupled sampling. Biophys Physicobiol 2020:BSJ-2020013.
56. Cao Y, Li L. Improved protein-ligand binding affinity prediction by using a curvature-dependent surface-area model. Bioinformatics 2014; 30(12):1674-1680.

57. Al Hosani FI, Pringle K, Al Mulla M, *et al*. Response to emergence of Middle East respiratory syndrome coronavirus, Abu dhabi, United Arab Emirates, 2013–2014. Emerg Infect Dis 2016; 22(7):1162.
58. Zhu N, Zhang D, Wang W, *et al*. A novel coronavirus from patients with pneumonia in China, 2019. New Engl J Med 2020;382(8):727-733.
59. Farzanegan MR, Feizi M, Gholipour HF. Globalization and the outbreak of COVID-19: An empirical analysis. J Risk Financ Manag 2021; 14(3):105.
60. Sanyaolu A, Okorie C, Marinkovic A, *et al*. The emerging SARS-CoV-2 variants of concern. Ther Adv Infect Dis 2021; 8:20499361211024372.
61. Landis MS, Long RW, Krug J, *et al*. The US EPA wildland fire sensor challenge: Performance and evaluation of solver submitted multi-pollutant sensor systems. Atmos Environ 2021; 247:118165.
62. Biccard BM, Gopalan PD, Miller M, *et al*. Patient care and clinical outcomes for patients with COVID-19 infection admitted to African high-care or intensive care units (ACCCOS): a multicentre, prospective, observational cohort study. Lancet 2021; 397(10288):1885-1894.
63. Allen WJ, Rizzo RC. Computer-aided approaches for targeting HIVgp41. Biology 2012; 1(2):311-338.
64. Yan R, Zhang Y, Li Y, *et al*. Structural basis for the recognition of SARS-CoV-2 by full-length human ACE2. Science 2020; 367(6485):1444-1448.
65. Wong CW, Albert TJ, Vega VB, *et al*. Tracking the evolution of the SARS coronavirus using high-throughput, high-density resequencing arrays. Genome Res 2004; 14(3):398-405.
66. Huang Y, Yang C, Xu X. feng, Xu, W., Liu, S.-wen, 2020. Structural and functional properties of SARS-CoV-2 spike protein: potential antivirus drug development for COVID-19. Acta Pharmacol Sin; 41:1141-1149.
67. Daina A, Michielin O, Zoete V. SwissADME: a free web tool to evaluate pharmacokinetics, drug-likeness and medicinal chemistry friendliness of small molecules. Sci Rep 2017; 7(1):1-13.
68. Pei K, Ou J, Huang J, *et al*. p-Coumaric acid and its conjugates: dietary sources, pharmacokinetic properties and biological activities. J Sci Food Agric 2016; 96(9):2952-2962.
69. Kheiry M, Dianat M, Badavi M, *et al*. p-Coumaric acid attenuates lipopolysaccharide-induced lung inflammation in rats by scavenging ROS production: an in vivo and in vitro study. Inflammation 2019; 42(6):1939-1950.
70. Tungmunnithum D, Thongboonyou A, Pholboon A, *et al*. Flavonoids and other phenolic compounds from medicinal plants for pharmaceutical and medical aspects: An overview. Medicines 2018; 5(3):93.
71. Ahmed SHH, Gonda T, Hunyadi A. Medicinal chemistry inspired by ginger: exploring the chemical space around 6-gingerol. RSC Advances 2021; 11(43):26687-26699.
72. Song F, Li H, Sun J, *et al*. Protective effects of cinnamic acid and cinnamic aldehyde on isoproterenol-induced acute myocardial ischemia in rats. J Ethnopharmacol 2013; 150(1):125-130.
73. Silveira D, Prieto-Garcia JM, Boylan F, *et al*. COVID-19: is there evidence for the use of herbal medicines as adjuvant symptomatic therapy? Front Pharmacol 2020; 11:1479.
74. Hashem H. In silico approach of some selected honey constituents as SARS-CoV-2 main protease (COVID-19) inhibitors. EJMO 4 (3)(2020) 196–200.
75. Wang J, Prinz RA, Liu X, *et al*. In vitro and in vivo antiviral activity of gingerenone A on influenza A virus is mediated by targeting janus kinase 2. Viruses 2020; 12(10):1141.
76. Lee HY, Park SH, Lee M, *et al*. 1-Dehydro-[10]-gingerdione from ginger inhibits IKKβ activity for NF-κB activation and suppresses NF-κB-regulated expression of inflammatory genes. Br J Pharmacol 2012; 167(1):128-140.
77. Kufareva I, Katritch V, Stevens RC, *et al*. Advances in GPCR modeling evaluated by the GPCR Dock 2013 assessment: meeting new challenges. Structure 2014; 22(8):1120-1139.
78. Matricon P, Suresh RR, Gao Z-G, *et al*. Ligand design by targeting a binding site water. Chem Sci 2021; 12(3):960-968.
79. Aier I, Varadwaj PK, Raj U. Structural insights into conformational stability of both wild-type and mutant EZH2 receptor. Sci Rep 2016; 6(1):1-10.
80. Sixto-López Y, Correa-Basurto J, Bello M, *et al*. Structural insights into SARS-CoV-2 spike protein and its natural mutants found in Mexican population. Sci Rep 2021; 11(1):1-16.